ELSEVIER
Chemical Geology 186 (2002) 315–331
CHEMICAL GEOLOGY
INCLUDING
ISOTOPE GEOSCIENCE
www.elsevier.com/locate/chemgeo

Constraints on timing of peak and retrograde metamorphism in the Dabie Shan Ultrahigh-Pressure Metamorphic Belt, east-central China, using U–Th–Pb dating of zircon and monazite

John C. Ayers [a,*], Stacie Dunkle [a], Shan Gao [b], Calvin F. Miller [a]

[a] *Department of Geology, Vanderbilt University, P.O. Box 105 Station B, Nashville, TN 37235 USA*
[b] *Key Laboratory of Continental Dynamics, Department of Geology, Northwest University, Xi'an 710069, China*

Accepted 18 January 2002

Abstract

The Dabie Shan Ultrahigh-Pressure Metamorphic (UHPM) Belt occupies the suture between the Yangtze and Sino-Korean blocks in east-central China. The timing of UHPM in the Dabie belt is controversial, and most recent data come from dating of zircons. Monazite has recently been recognized as useful for dating of multiple tectonic events due to its preservation of multiple growth zones, and monazite growth has been documented to occur during prograde, peak, and retrograde metamorphism. Zircons and monazites from UHP mafic rocks from Maowu and a UHP jadeite quartzite from Shuanghe were imaged in thin sections and in mineral separates and dated using a high-resolution ion microprobe. Maowu mafic rocks are unique in that they contain high light rare earth element concentrations and therefore contain abundant monazite. Maowu eclogites and garnet pyroxenites contain zircons with mean $^{206}Pb/^{238}U$ age of $\sim 230 \pm 4$ Ma, and monazites from a clinopyroxenite have $^{208}Pb/^{232}Th$ ages of $\sim 209 \pm 4$ Ma. Multiple lines of evidence suggest that the measured ages represent the timing of new growth and recrystallization and are not cooling ages (i.e., they do not correspond to the cessation of diffusional Pb loss as rocks cooled below the closure temperature during exhumation). Shuanghe jadeite quartzites contain zircons with cores that define a discordia with an upper intercept age 1921 ± 22 Ma and lower intercept age of 236 ± 32 Ma, interpreted to represent the ages of the source rocks and of peak metamorphism, respectively. Zircon rims contain jadeite inclusions that restrict growth to pressures greater than 1.5 GPa. Their pooled age of 238 ± 3 Ma agrees well with the lower intercept defined by cores, suggesting that Pb loss from cores and growth of new rims occurred during UHPM at $\sim 235–240$ Ma. Monazite records multiple events during retrograde metamorphism. Maowu clinopyroxenite and Shuanghe jadeite quartzite experienced monazite growth at ~ 209 Ma, interpreted to reflect regional amphibolite facies overprinting resulting from pervasive retrograde fluid infiltration. Only the jadeite quartzite records growth at 223 ± 1 Ma. Estimated exhumation rates for Maowu are 7–8 km/Ma. © 2002 Elsevier Science B.V. All rights reserved.

Keywords: Metamorphism; Monazite; Zircon; Geochronology; Dabie Mountains; Ion probe dating

1. Introduction

In the last 10 years, many studies have focused on Ultrahigh-Pressure Metamorphism (UHPM) of crustal rocks. Pressures exceeding those defined by the quartz-coesite transition characterize UHPM, so the presence

* Corresponding author. Tel.: +1-615-322-2158; fax: +1-615-322-2138.
E-mail address: john.c.ayers@vanderbilt.edu (J.C. Ayers).

PII: S0009-2541(02)00008-6

of coesite or other UHP index minerals, such as diamond, that are stable at even higher pressures is evidence of UHPM (Liou et al., 1998). Typically, these UHP minerals are found as inclusions in garnet or zircon in eclogites and garnet peridotites that occur as pods and slabs in quartzofeldspathic gneisses. UHP terranes lie within major continental Alpine-type Phanerozoic collision belts. They are typically thin, bounded by faults, and adjacent to high-pressure or lower grade units. Arc-related and syn-collisional rocks are generally absent, but post-collisional granites are common (Ernst et al., 1997).

The Dabie–Sulu Terrane in east-central China is the largest UHP belt in the world. It occupies a suture formed by Triassic collision between the passive northern margin of the Yangtze (South China) craton with the active southern margin of the Sino-Korean (North China) craton (Liou et al., 1996). Rocks in the Dabie–Sulu terrane have received much attention because they contain the lowest δ^{18}O rocks recorded on earth; the highest $P-T$ equilibration conditions yet recorded, corresponding to conditions in the "Forbidden Zone" of geothermal gradients < 5 °C/km (Liou et al., 2000); diamonds (Xu et al., 1992); abundant coesite and hydrous phases (talc, zoisite/epidote, phengite); and abundant mantle-derived garnet peridotites (Liou et al., 1998).

The Dabie Shan lie at the eastern end of the ~ 3000-km-long Kunlun–Qilian–Qinling–Dabie orogenic belt (inset of Fig. 1). The Sulu UHP belt appears to be equivalent to this belt, but is offset ~ 530 km to the north by the Tan-Lu fault (Hacker et al., 1998). The Dabie Shan are bounded by the Shang-Ma Fault to the west (not shown), the Tan-Lu Fault to the east, and the Xiaotian-Mozitan Fault to the north (Fig. 1), and consist of three principal units: the northern Dabie Shan, a high-T magmatic terrane with abundant post-collisional Cretaceous granitoids that intrude the North Dabie Complex, which is dominated by amphibolite-facies tonalitic and trondhjemitic gneisses (Ratschbacher et al., 2000); a central UHP coesite- and diamond-bearing eclogite belt (P = 2.6–6.5 GPa); and a southern HP metamorphic belt (P = 0.5–2.1 GPa).

In the central Dabie UHP zone, eclogites and paragneisses preserve evidence of UHPM while orthogneisses do not. This observation led to the "foreign source" model, which stated that only isolated blocks of eclogite and paragneiss experienced UHPM before tectonic intercalation with host orthogneisses. The competing in situ model posits that the entire central

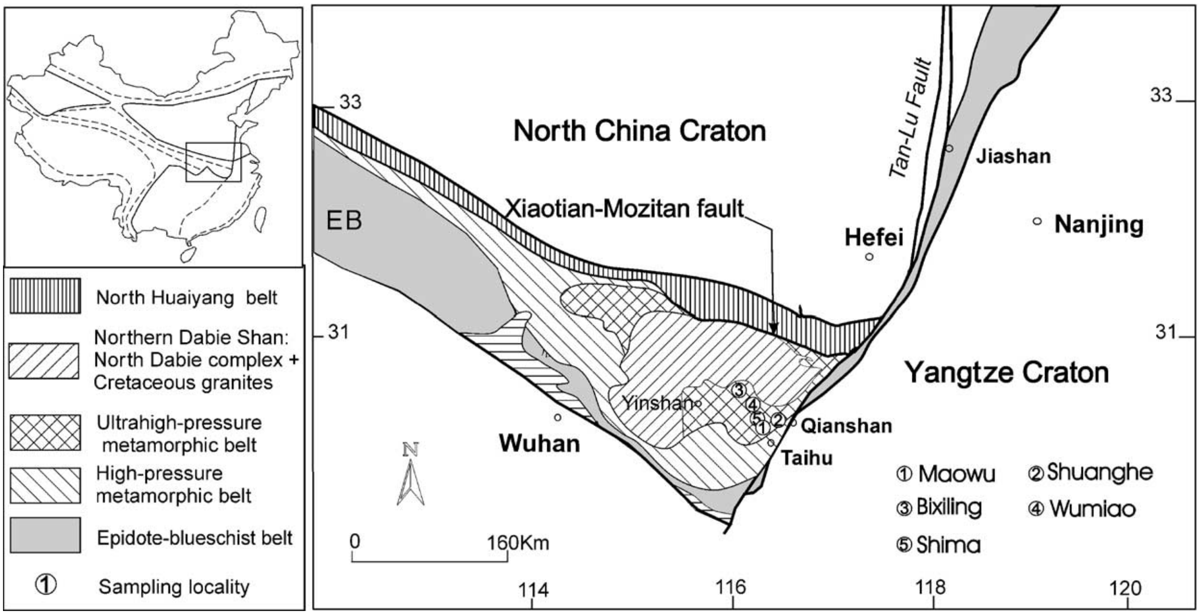

Fig. 1. Map showing location of Maowu and Shuanghe sampling sites and regional setting of Dabie Shan UHPM belt.

Table 1
Zircon U/Pb data for analyzed spots

Analysis[a]	$^{206}Pb^{b}/^{238}U$	2σ	$^{207}Pb^{b}/^{235}U$	2σ	Age (Ma) $^{206}Pb/^{238}U$	2σ	Age (Ma) $^{207}Pb/^{235}U$	2σ	Age (Ma) $^{207}Pb/^{206}Pb$	2σ	% Rad. $^{206}Pb^{c}$	U conc. (ppm)
Sh-JQ-z-01-sp1-R	0.0374	0.0018	0.2476	0.1144	237	11	225	93	102	1032	95.1	350
Sh-JQ-z-01-sp2-R	0.0383	0.0013	0.2768	0.1058	242	8	248	84	304	828	95.7	332
Sh-JQ-z-03-sp1-C	0.2097	0.0038	3.2060	0.0534	1227	21	1459	13	1815	17	99.9	1595
Sh-JQ-z-03-sp2-C	0.0416	0.0015	0.3518	0.0616	263	10	306	46	651	350	97.7	438
Sh-JQ-z-06-sp1-C	0.2761	0.0087	4.4230	0.1574	1572	44	1717	29	1898	21	99.9	742
Sh-JQ-z-08-sp1-C	0.2467	0.0060	3.8140	0.0946	1422	31	1596	20	1834	13	99.9	1782
Sh-JQ-z-10-sp1-C	0.1681	0.0040	2.5580	0.0712	1002	22	1289	20	1806	17	99.9	986
Sh-JQ-z-10-sp2-R	0.0363	0.0017	0.2458	0.0916	230	11	223	75	153	822	96.1	356
Sh-JQ-z-15-sp1-C	0.2645	0.0070	4.2710	0.1292	1513	36	1688	25	1913	14	99.9	986
Sh-JQ-z-22-sp1-R	0.0374	0.0013	0.2549	0.0774	236	8	231	63	172	660	96.7	312
Sh-JQ-z-25-sp1-R	0.0377	0.0008	0.2693	0.0218	238	5	242	18	279	170	99.1	1542
Sh-JQ-z-25-sp2-C	0.0609	0.0017	0.6390	0.0358	381	10	502	22	1098	87	99.3	866
Sh-JQ-z-25-sp3-C	0.0429	0.0008	0.3748	0.0154	271	5	323	11	723	68	99.5	1572
Sh-JQ-z-28-sp1-C	0.1616	0.0035	2.3960	0.0846	966	20	1241	25	1758	41	99.7	933
Sh-JQ-z-28-sp2-R	0.0378	0.0018	0.2925	0.0504	239	11	261	40	460	340	97.4	314
Sh-JQ-z-33-sp1-C	0.2088	0.0047	3.2360	0.0770	1223	25	1466	18	1838	12	99.9	1631
Sh-JQ-z-33-sp2-C	0.1131	0.0030	1.5960	0.0980	691	18	969	38	1667	107	99.3	647
Sh-JQ-z-36-sp1-C	0.2215	0.0041	3.4470	0.0780	1290	22	1515	18	1846	19	99.9	1447
MAO-MW2-z-04-sp1-C	0.0333	0.0049	0.2233	0.5040	211	31	205	418	133	5140	60.3	28
MAO-MW2-z-04-sp2-R	0.0365	0.0043	0.2040	0.3620	231	27	189	306	0	0	83.3	84
MAO-MW2-z-08-sp1-C	0.0390	0.0068	0.1052	0.5500	247	42	102	504	0	0	75.8	69
MAO-MW2-z-08-sp2-C	0.0359	0.0040	0.2864	0.2560	227	25	256	202	524	1850	87.5	114
MAO-MW2-z-08-sp3-R	0.0360	0.0030	0.2371	0.2520	228	19	216	206	90	2420	87.0	89
MAO-MW2-z-14-sp1-C	0.0361	0.0022	0.2159	0.1520	229	14	199	127	0	0	93.3	200
MAO-MW2-z-14-sp2-R	0.0354	0.0037	0.1778	0.2780	224	23	166	240	0	0	89.3	140
MAO-MW2-z-14-sp3-R	0.0360	0.0018	0.2357	0.1440	228	11	215	118	74	1386	93.3	284
MAO-MW2-z-24-sp1-C	0.0363	0.0053	0.3577	0.4900	230	33	311	366	969	2640	79.6	49
MAO-MW2-z-24-sp2-R	0.0371	0.0009	0.2585	0.0360	235	6	234	29	220	298	98.5	751
MAO-MW2-z-24-sp3-R	0.0368	0.0032	0.2406	0.2380	233	20	219	194	73	2240	88.0	85
MAO-MWA3-z-46-sp2-R	0.0347	0.0024	0.2069	0.0716	220	15	191	60	0	0	95.4	105
MAO-MWA3-z-51-sp1-C	0.0404	0.0023	0.1162	0.1150	256	14	112	105	0	0	89.2	146
MAO-MWA3-z-51-sp2-R	0.0360	0.0022	0.2408	0.1242	228	14	219	102	124	1174	92.2	90
MAO-MWA3-z-56-sp1-C	0.0371	0.0021	0.2195	0.0870	235	13	202	72	0	0	95.4	169
MAO-MWA3-z-56-sp2-R	0.0346	0.0023	0.2002	0.1592	219	14	185	135	0	0	90.6	87
MAO-MWA3-z-68-sp1-R	0.0362	0.0019	0.2530	0.1000	229	12	229	81	229	868	95.1	113
MAO-MWA4-z-39-sp1-R	0.0359	0.0037	0.2249	0.2480	227	23	206	206	0	0	84.9	80
MAO-MWA4-z-39-sp2-C	0.0344	0.0023	0.2268	0.0590	218	14	208	49	93	530	98.6	594
MAO-MWB2-z-100-sp1-C	0.0367	0.0050	0.2840	0.3740	232	31	254	296	456	2800	79.2	24
MAO-MWB2-z-100-sp2-R	0.0330	0.0034	0.2663	0.1902	209	21	240	152	552	1466	89.5	38
MAO-MWB2-z-70-sp1-C	0.0379	0.0027	0.1878	0.1672	240	17	175	143	0	0	88.9	46
MAO-MWB2-z-70-sp2-R	0.0355	0.0029	0.2562	0.1742	225	18	232	141	299	1472	91.2	43
MAO-MWB2-z-80-sp1-C	0.0369	0.0017	0.2505	0.0782	234	11	227	63	160	682	96.6	180
MAO-MWB2-z-80-sp2-R	0.0357	0.0015	0.2899	0.1042	226	9	259	82	563	732	95.6	209
MAO-MWB2-z-82-sp2-R	0.0374	0.0039	0.2788	0.1000	237	24	250	79	372	746	93.6	49

[a] Each analysis represents a single spot on a zircon; label represents location-sample-mineral-grain number-spot number-core/rim; Mao = Maowu, Sh = Shuanghe, MW2 and MWB2 are eclogites, MWA3 is a garnet pyroxenite, MWA4 is a garnet orthopyroxenite.

[b] Radiogenic Pb, corrected for common Pb. ^{208}Pb correction used for all analyses except for jadeite quartzite zircon cores, which used ^{204}Pb correction (see text).

[c] % Radiogenic ^{206}Pb calculated from uncorrected $^{206}Pb/^{204}Pb$ ratios; common Pb ratios used in correction: $^{206}Pb/^{204}Pb = 18.350$ and $^{207}Pb/^{204}Pb = 15.611$, except for cores on JQ for which common Pb ratios were $^{206}Pb/^{204}Pb = 15.365$ and $^{207}Pb/^{204}Pb = 15.241$.

zone experienced UHPM as an intact unit, and subsequent retrograde metamorphism obliterated all evidence of UHPM from the orthogneisses (Liou et al., 1996). Different levels of fluid activity probably determined the different responses to UHP and retrograde metamorphism. Recent evidence supporting the in situ model includes coesite inclusions in zircons from amphibolite-facies orthogneisses in Dabie Shan (Tabata et al., 1998) and Sulu (Ye et al., 2000) and geochronologic evidence that eclogites and host orthogneisses in central Dabie Shan share a common history (Rowley et al., 1997; Hacker et al., 1998; Li et al., 2000).

The timing of peak UHPM is most reliably dated by zircon U/Pb analysis. Previous studies (see summary in Hacker et al., 2000) show that zircons from Dabie Shan commonly have Precambrian cores, ~ 625–800 Ma in age. They also have metamorphic rims with a range of measured ages from 205 ± 5 to 248 ± 7 Ma with broad, poorly defined peaks at ~ 230, 218 and 209 Ma. Hacker et al. (2000) interpret the ~ 230–240 Ma ages to represent peak UHPM and younger ages as representing post-UHP growth.

The cooling and exhumation history of the Dabie Shan UHP metamorphic belt is only now becoming established and it places important constraints on exhumation processes and the tectonic history of this terrane. Sm–Nd and Rb–Sr mineral isochrons from eclogites and host orthogneisses in the central UHP zone show a shared cooling history, supporting the in situ model (Li et al., 2000). UHP minerals (garnet, omphacite, phengite) define Sm–Nd isochron ages of 226 ± 3 Ma, interpreted to represent peak metamorphism. Retrogressed minerals (epidote, amphibole, biotite, plagioclase) in the matrix of eclogite and orthogneiss typically define younger isochrons than those defined by UHP minerals. Both trace element and isotopic evidence suggest that infiltration of fluid at 213 ± 3 Ma during retrograde metamorphism in the amphibolite facies added Rb, Nd with a lower ^{143}Nd/^{144}Nd, and Sr with a higher ^{87}Sr/^{86}Sr than in the unaltered rock (Li et al., 2000). Similarly, Hacker et al. (1998) attributed growth of zircon rims in Dabie Shan granitoids at ~ 219 Ma to retrograde fluid activity. Combining P–T–t information from peak and retrogressed assemblages leads to estimates of exhumation rates of > 2 km/Ma (Hacker et al., 2000) and cooling rates of ~ 40°/Ma (Li et al., 2000).

Table 2
Monazite Pb/U data for analyzed spots

Analysis[a]	^{208}Pb*/^{232}Th	% Rad. ^{208}Pb[b]	Age (Ma)	2σ
Mao-MWA5-m-53-sp1-C-2	0.01065	93.7	214	2
Mao-MWA5-m-53-sp2-R-2	0.01031	96.1	207	2
Mao-MWA5-m-59-sp1-NA-2	0.01024	96.9	206	1
Mao-MWA5-m-59-sp2-NA-2	0.01042	95.7	210	2
Mao-MWA5-m-59-sp3-NA-2	0.01030	97.6	207	2
Mao-MWA5-m-63-sp1-C-2	0.01042	95.6	210	2
Mao-MWA5-m-63-sp2-R-2	0.01045	96.7	210	2
Mao-MWA5-m-64-sp1-C-2	0.01052	95.5	212	2
Mao-MWA5-m-64-sp2-R-2	0.01017	97.0	204	1
Mao-MWA5-m-65-sp1-R-2	0.01009	94.6	203	2
Mao-MWA5-m-65-sp2-C-2	0.01051	94.1	211	2
Mao-MWA5-m-68-sp1-NA-2	0.01066	88.8	214	2
Mao-MWA5-m-68-sp2-NA-2	0.01064	97.3	214	1
Mao-MWA5-m-69-sp1-C-2	0.01064	95.8	214	2
Mao-MWA5-m-69-sp2-R-2	0.01076	97.1	216	2
Mao-MWA5-m-71-sp1-C-2	0.01047	88.7	211	2
Mao-MWA5-m-71-sp2-R-2	0.01064	97.9	214	2
Mao-MWA5-m-74-sp1-C-2	0.01059	96.2	213	2
Mao-MWA5-m-74-sp2-R-2	0.01044	96.8	210	2
Mao-MWA5-m-76-sp1-C-2	0.01033	93.9	208	2
Mao-MWA5-m-76-sp2-R-2	0.01039	96.8	209	1
Mao-MWCTS-m-01-sp1-NA-2	0.00998	94.5	201	2
Mao-MWCTS-m-01-sp2-NA-2	0.01021	96.4	205	2
Mao-MWCTS-m-02-sp1-NA-2	0.01022	95.8	205	2
Mao-MWCTS-m-03-sp1-NA-2	0.01004	91.8	202	2
Sh-JQ-03-sp1-R-1	0.01109	99.2	223	1
Sh-JQ-m-03-sp2-C-1	0.01128	99.3	227	2
Sh-JQ-m-09-sp1-NA-2	0.01046	98.9	210	2
Sh-JQ-m-10-sp1-NA-1	0.01115	99.2	224	2
Sh-JQ-m-12-sp1-NA-2	0.01008	99.1	203	2
Sh-JQ-m-12-sp2-NA-2	0.01035	99.0	208	2
Sh-JQ-m-18-sp1-NA-1	0.01107	99.2	223	2
Sh-JQ-m-18-sp2-NA-1	0.01113	99.2	224	2
Sh-JQ-m-27-sp1-C-1	0.01118	99.2	225	2
Sh-JQ-m-27-sp2-R-2	0.01062	99.0	213	2
Sh-JQ-m-32-sp1-C-1	0.01115	99.2	224	3
Sh-JQ-m-32-sp2-R-2	0.01033	98.9	208	1
Sh-JQ-m-37-sp1-C-1	0.01103	98.9	222	2
Sh-JQ-m-37-sp2-R-2	0.01030	99.0	207	2
Sh-JQ-m-40-sp1-NA-1	0.01110	99.1	223	2
Sh-JQ-m-40-sp2-NA-1	0.01107	99.1	223	2
Sh-JQ-m-40-sp3-NA-2	0.01061	99.0	213	2
Sh-JQ-m-41-sp1-C-1	0.01096	99.2	220	3
Sh-JQ-m-41-sp2-R-2	0.01023	99.0	206	1
Sh-JQ-m-47-sp1-C-1	0.01106	99.2	222	2
Sh-JQ-m-47-sp2-R-2	0.01059	99.0	213	2

[a] Label represents sample location-sample (rock type)-mineral-grain number-spot #-core/rim-generation. Sh = Shuanghe, Mao = Maowu; JQ = Jadeite quartzite, MWA5 clinopyroxenite separate, MWCTS clinopyroxenite thin section, m = monazite, C = core, R = rim, NA = not applicable.

[b] % Radiogenic ^{208}Pb calculated from uncorrected ^{208}Pb/^{204}Pb ratios. Common Pb ratio used in correction: ^{208}Pb/^{204}Pb = 36.7.

Table 3
Summary of results

Location	Lithology	Zircon		Monazite	
		Age and 2σ error (Ma)	Comments	Age and 2σ error (Ma)	Comments
Shuanghe	Jadeite quartzite	1921 ± 23	Discordia upper int.;	223 ± 1	$^{208}Pb/^{232}Th$ spot, cores
		236 ± 32	Discordia lower int.	209 ± 3	$^{208}Pb/^{232}Th$ spot, rims
		238 ± 3	$^{206}Pb/^{238}U$ spot		
Maowu	Eclogite	232 ± 3	$^{206}Pb/^{238}U$ spot		
	Garnet pyroxenite	227 ± 5	$^{206}Pb/^{238}U$ spot		
	Clinopyroxenite			209 ± 2	pooled $^{208}Pb/^{232}Th$ spot
				209 ± 4	$^{208}Pb/^{232}Th$ inverse isochron

Infiltration of fluids during retrograde metamorphism is likely to cause monazite recrystallization in addition to new growth of zircon. Monazite is a potentially powerful monitor of fluid activity during UHP metamorphism because hydrothermal dissolution–reprecipitation has been shown to reset the monazite

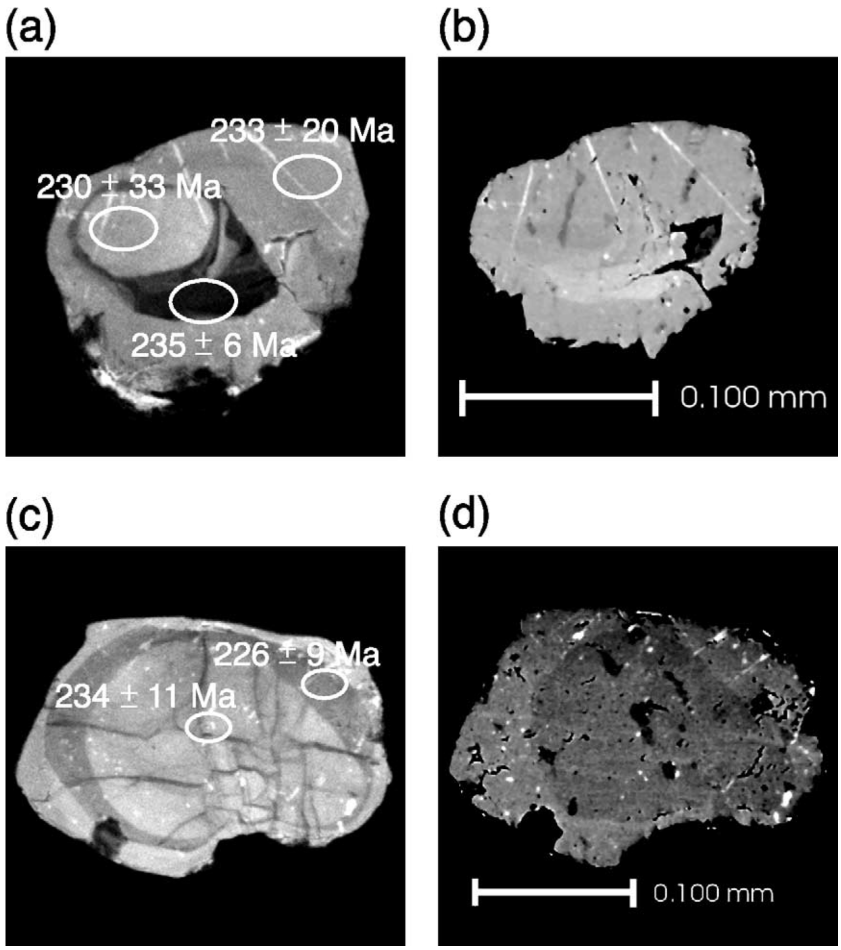

Fig. 2. Zircons from Maowu eclogite. Images (a)–(b) and (c)–(d) are paired cathodoluminescence and backscattered electron (BSE) images of grains MAO-MW2-Z-24 and MAO-MWB2-Z-80, respectively. Scalebars are shown on the BSE images. Ellipses mark analysis spots labeled with measured ages and associated 2σ errors.

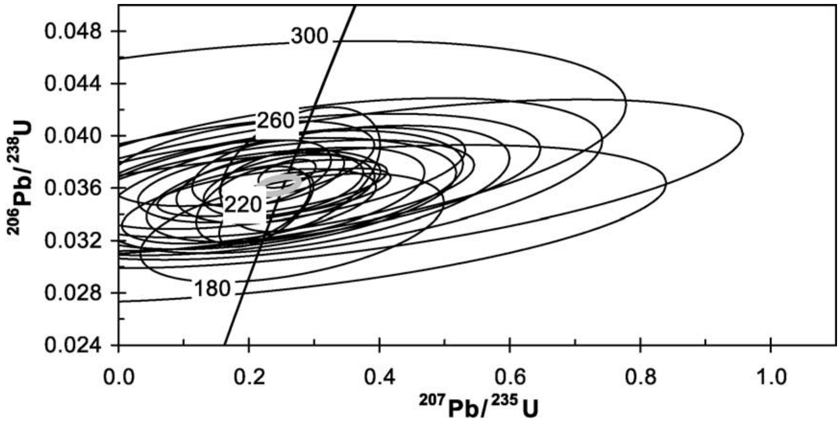

Fig. 3. Twenty-five analyses of Maowu zircons plotted on a concordia diagram; uncertainty ellipses are $\pm 2\sigma$. Concordia age = 229.6 ± 2.6 Ma (2σ), with MSWD of concordance = 0.71. Grey-shaded ellipse represents the weighted mean.

U, Th/Pb isotopic systems (Townsend et al., 2000; Crowley and Ghent, 1999; Poitrasson et al., 1996; Fitzsimmons et al., 1997; Teufel and Heinrich, 1997; Hawkins and Bowring, 1997). Zoned monazites with patchy zones and veins indicative of fluid-assisted partial recrystallization commonly occur in granitoids; ion microprobe dating of the recrystallized zones gives the age of fluid infiltration (e.g., Townsend et al., 2000). However, monazites in Dabie Shan rocks have not been dated prior to this study.

This study presents results from high-resolution ion microprobe analyses of zircon and monazite from two well-studied sites in the central Dabie UHP zone. The objective was to compare the different responses of

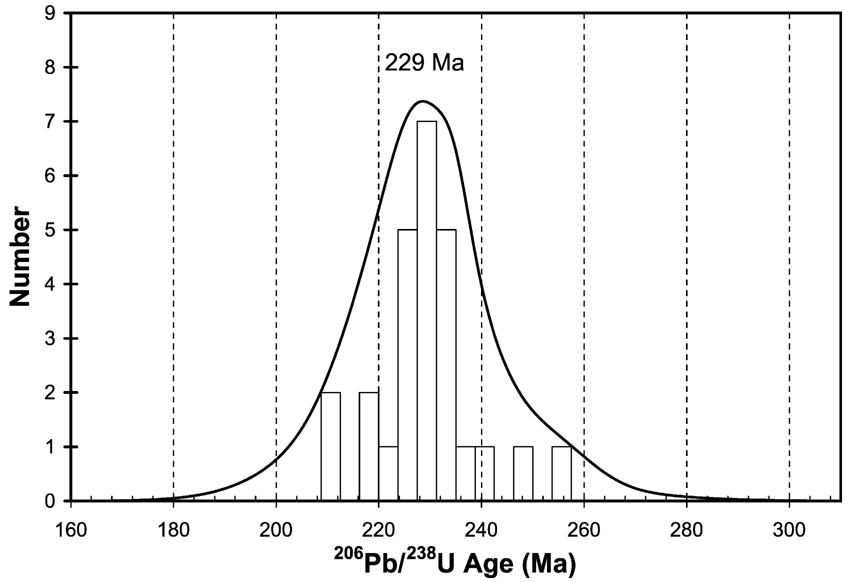

Fig. 4. Histogram of measured $^{206}Pb/^{238}U$ ages of Maowu zircons. Solid line represents the cumulative probability obtained by summing the probability distributions of all analyses assuming measurement errors are normally distributed (Deino and Potts, 1992).

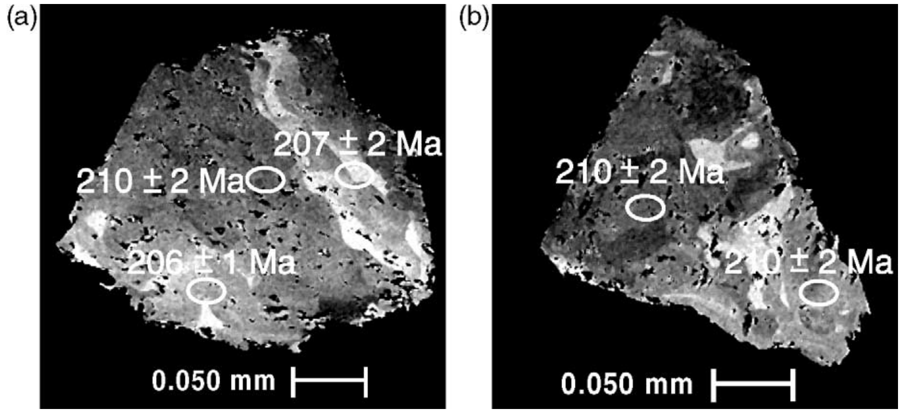

Fig. 5. BSE images of monazites from Maowu clinopyroxenite: (a) MAO-MWA5-M-59; and (b) MAO-MWA5-M-63. Ellipses mark analysis spots labeled with measured ages and their 2σ errors.

zircon and monazite to UHPM in rocks with well-characterized $P-T$ paths, and to combine the two sets of information to obtain $P-T-t$ paths and exhumation rates.

2. Sample localities

The Maowu mafic body (location in Fig. 1) is described in detail by Liou and Zhang (1998). It measures $\sim 250 \times >50$ m and contains layers of eclogite and garnet orthopyroxenites with minor harzburgite and omphacite-rich (clinopyroxenite) layers. The entire body, particularly the clinopyroxenite layers, is enriched in light rare earth elements, and monazite ($REEPO_4$) and zircon are found as inclusions in silicates and as a matrix phase. Based on petrography, thermobarometry and stable isotopes, the Maowu mafic body is inferred to have a complex history of: (1) differentiation of gabbroic magma in the Proterozoic to form a crustal layered-cumulate complex; (2) addition of meteoric water that added REE and imparted a depleted $\delta^{18}O$

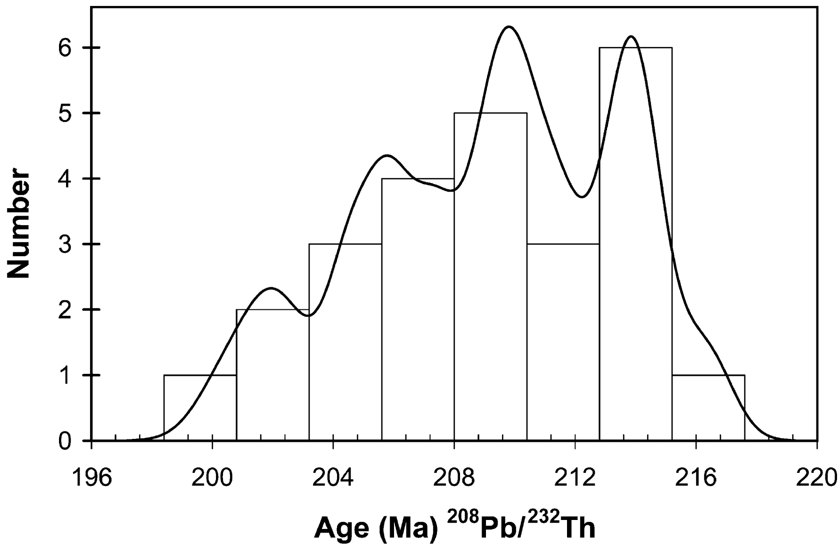

Fig. 6. Cumulative probability plot, with histogram, of measured $^{208}Pb/^{232}Th$ ages of Maowu clinopyroxenite monazites.

signature; (3) tectonic emplacement in a quartzofeldspathic + carbonate sequence; (4) subduction to depths >100 km (P = 3.5–5.0 GPa, T = 750 ± 50 °C); and (5) exhumation with the surrounding UHPM terrane. Sr and Nd isotope systematics suggest that Maowu eclogite was derived from long-term enriched mantle or experienced crustal contamination (Jahn, 1998). Zircons from the Maowu eclogite dated previously by TIMS showed slight discordance, defining a lower intercept age of 225.5 + 3/ − 6 Ma and an upper intercept age of 447 + 82/ − 79 Ma (Rowley et al., 1997).

Coesite-bearing jadeite quartzite collected from the Shuanghe UHP slab (located in Fig. 1 and described by Liou et al., 1997) contains abundant zircon and rare but relatively large (~ 200 μm) monazite grains. The peak metamorphic assemblage is jadeite + garnet + coesite + rutile ± apatite. Its clockwise P–T path is similar to that of adjacent coesite-bearing eclogites and other UHP rocks in Dabie Shan, with peak metamorphic conditions of >2.6 GPa and 660 °C. Retrograde metamorphism produced kelyphitic overgrowths on jadeite porphyroblasts consisting of plagioclase, amphibole and aegirine-augite. The source rock may have been albitized sandstone, and ε_{Nd} of − 24.7 and model age (T_{DM}) of 2.58 Ga suggest it was derived from the Archean crust (Liou et al., 1997).

3. Analytical techniques

Fresh samples were collected and crushed and standard mineral separation techniques were used to extract monazite and zircon crystals. Twenty to sixty grains from each sample, 50–300 μm in diameter, were mounted with standards in epoxy and then polished and imaged by backscattered electrons and cathodoluminescence using a Cameca SX-50 electron microprobe at the University of Tennessee at Knoxville. Internal zoning revealed by these images guided our choice of 15 × 20-μm analysis spots for high-resolution ion microprobe analysis using the Cameca ims1270 at the University of California at Los Angeles. Three monazite crystals in a 2.5-cm diameter thin section were also analyzed. Procedures follow those of Quidelleur et al. (1997) and Miller et al. (2000). Because zircon metamorphic rims are relatively young and typically have low Th concentrations, a high proportion of ^{208}Pb is common (Marayuma et al., 1998); therefore, the common Pb correction was based on

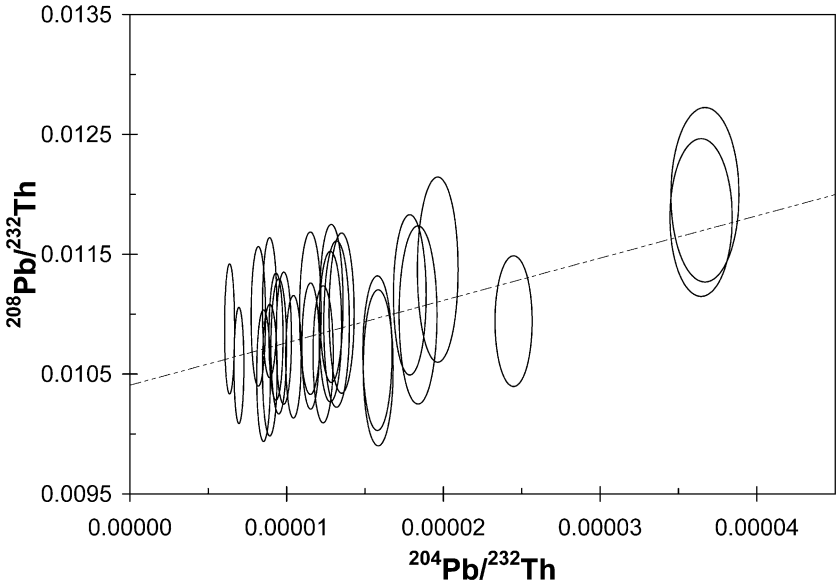

Fig. 7. Inverse ^{208}Pb/^{232}Th isochron for Maowu clinopyroxenite monazites. An inverse isochron requires no assumptions about error correlations. The age determined from the intercept is 209 ± 4 Ma, MSWD = 0.74.

^{208}Pb. For older zircon cores, ^{204}Pb was used for common Pb correction. Common Pb ratios at the determined age of the rock were estimated using the model of Stacey and Kramers (1975). For monazite, correction using ^{204}Pb had a small effect on the ^{208}Pb/^{232}Th age because the percentage of radiogenic ^{208}Pb was high (~ 99% in Shuanghe and ~ 95% in Maowu). U concentrations in zircons were estimated semiquantitatively by comparing values of $UO+/ZrO_2$ measured in unknowns to those measured in standard AS3, which has a mean concentration of 374 ppm (Miller et al., 2000). Reported ages are ^{206}Pb/^{238}U for zircon rims, ^{207}Pb/^{206}Pb for zircon cores, and ^{208}Pb/^{232}Th for monazite with mean and 95% confidence intervals (CI) or 2σ errors calculated by pooling multiple analyses, assuming a single population and weighting individual analyses by their inverse variance using the Isoplot program (Ludwig, 2000).

4. Analytical results

Table 1 contains zircon U/Pb data for spots analyzed using the high-resolution ion microprobe, Table 2 lists monazite Th/Pb data, and Table 3 summarizes age estimates for monazite and zircon.

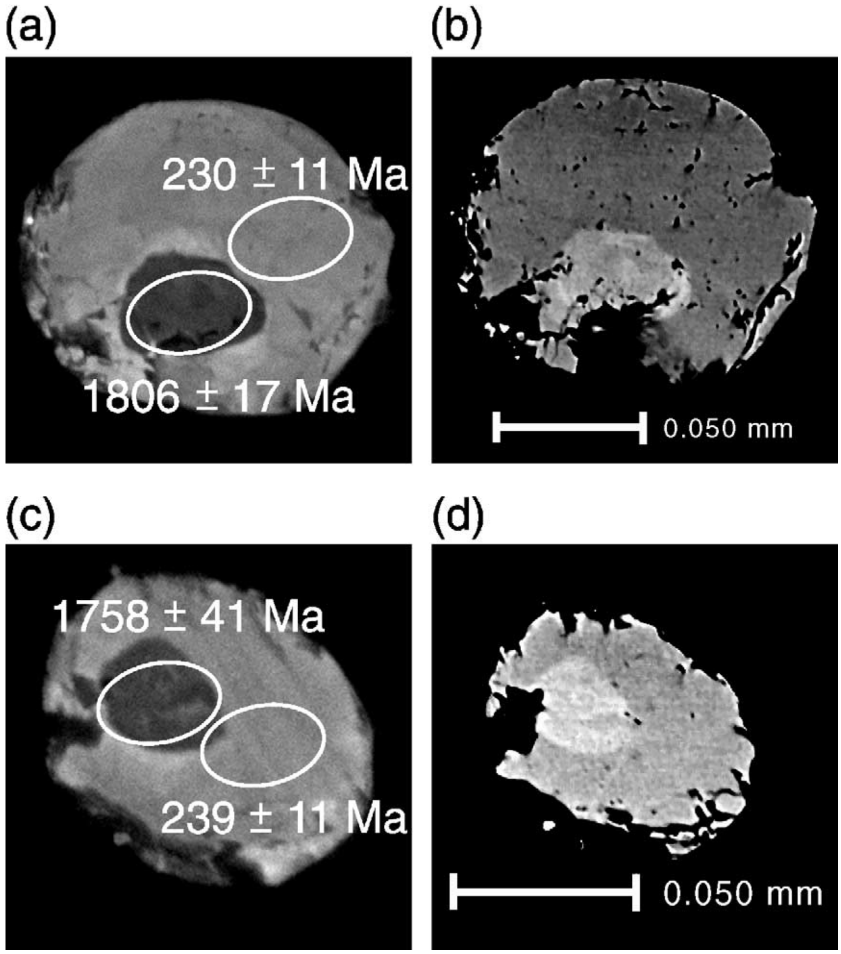

Fig. 8. Zircons from Shuanghe jadeite quartzite. Images (a)–(b) and (c)–(d) are paired cathodoluminescence and backscattered electron (BSE) images of SH-JQ-Z-10 and SH-JQ-Z-28, respectively. Scalebars are shown on the BSE images. Ellipses mark analysis spots labeled with measured ages (^{206}Pb/^{238}U for rims, ^{207}Pb/^{206}Pb for cores) and associated 2σ errors.

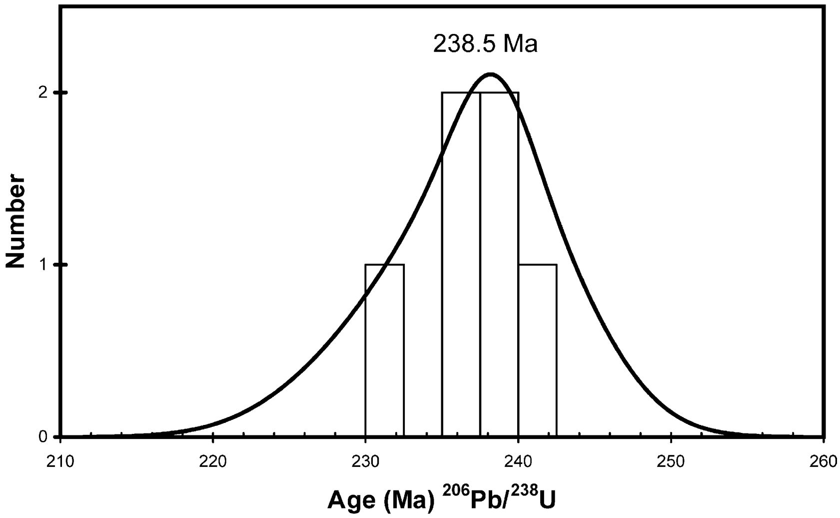

Fig. 9. Cumulative probability plot of measured $^{206}Pb/^{238}U$ ages of Shuanghe jadeite quartzite zircon rims. Mean age weighted by data point errors is 238 ± 3 Ma (95% CI), MSWD = 0.72.

4.1. Maowu

4.1.1. Zircons

Zircons from Maowu eclogite and garnet pyroxenite range in diameter from ~ 50 to 300 μm and do not exhibit well-developed crystal faces. They tend to be rounded but in some cases are angular or have embayments. Internal zoning is subtle in backscattered electron images but shows up well in cathodoluminescence (Fig. 2), with grains typically containing cores and one

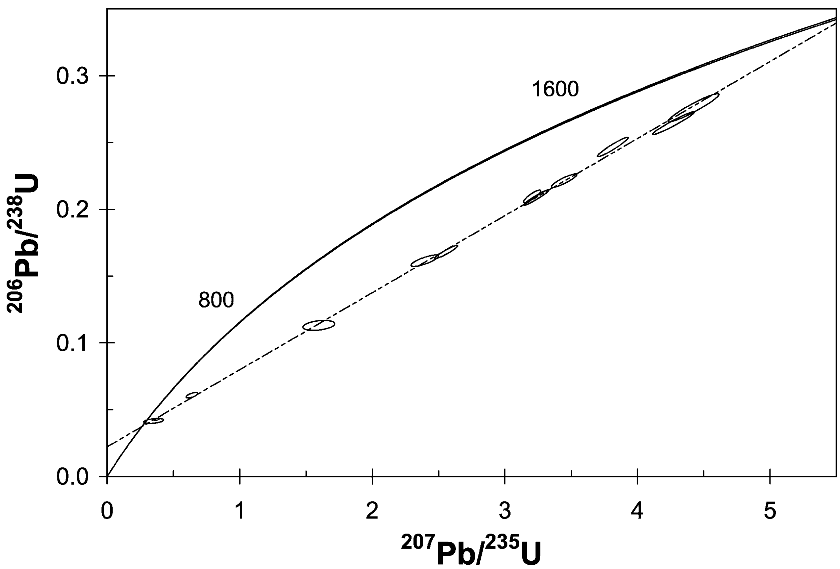

Fig. 10. Concordia diagram showing discordia defined by cores in jadeite quartzite zircons. Uncertainty ellipses are ± 2σ. Intercepts at 236 ± 32 and 1921 ± 22 Ma, with MSWD = 7.0. See text for interpretation.

or two thin rims. Some grains have no distinguishable cores but display subtle patchy zoning.

Uranium concentrations range from ~ 30 to 600 ppm, with no significant difference between median values for cores (110 ppm) and rims (100 ppm) (Table 1). Percent radiogenic ^{206}Pb averages 86% in cores and 91% in rims. Most analyses are concordant within 2σ uncertainty (Fig. 3), with no significant difference in age between cores (231 ± 5 Ma 95% CI, $n = 10$) and rims (229 ± 3 Ma, $n = 15$) or between zircon ages from eclogite (232 ± 3 Ma) and garnet pyroxenite (227 ± 5 Ma). Pooling core and rim ages yields a mean value of 230.6 ± 2.8 Ma, with the peak in a cumulative probability plot (Deino and Potts, 1992; Ludwig, 2000) at 229 Ma (Fig. 4). A previous TIMS study of zircon from Maowu yielded a poorly defined upper intercept at 447 + 82/ − 79 Ma (Rowley et al., 1997), but we found no evidence for such an older component.

4.1.2. Monazites

Monazites are rare in eclogite but more abundant in clinopyroxenite, where they occur as irregularly shaped yellow crystals 50–400 μm in diameter. In backscattered electron images, monazites from Maowu clinopyroxenite often have chaotic (patchy) zoning patterns (Fig. 5), but some have cores that are rounded, truncated, embayed, or irregularly shaped. These textures suggest that the monazites either partially or completely recrystallized, probably in the presence of a fluid. Radiogenic ^{208}Pb averaged 95% (Table 2). Most analyses were on separates, but we collected four analyses from three monazite grains in a thin section.

Based on analysis of grains from separates that showed clear core–rim zoning, cores (211 ± 2 Ma, $n = 8$) are not significantly older than the rims (209 ± 4 Ma, $n = 8$). Pooling ages of cores, rims and unclassified samples (those analyses from grains with no obvious core–rim zoning, $n = 25$) yields an age of 209.2 ± 1.8 Ma. The age probability plot shows a spread in measured ages from 200 to 216 Ma, slightly skewed to younger ages with one or more peaks between 208 and 215 Ma (Fig. 6). A $^{208}Pb/^{232}Th$ inverse isochron defines an age of 209 ± 4 Ma with MSWD = 0.74 (Fig. 7). We conclude that monazites from Maowu samples define a single population with a mean age of ~ 209 Ma, though recrystallization/growth may have occurred continuously or at discrete but closely spaced intervals over several million years.

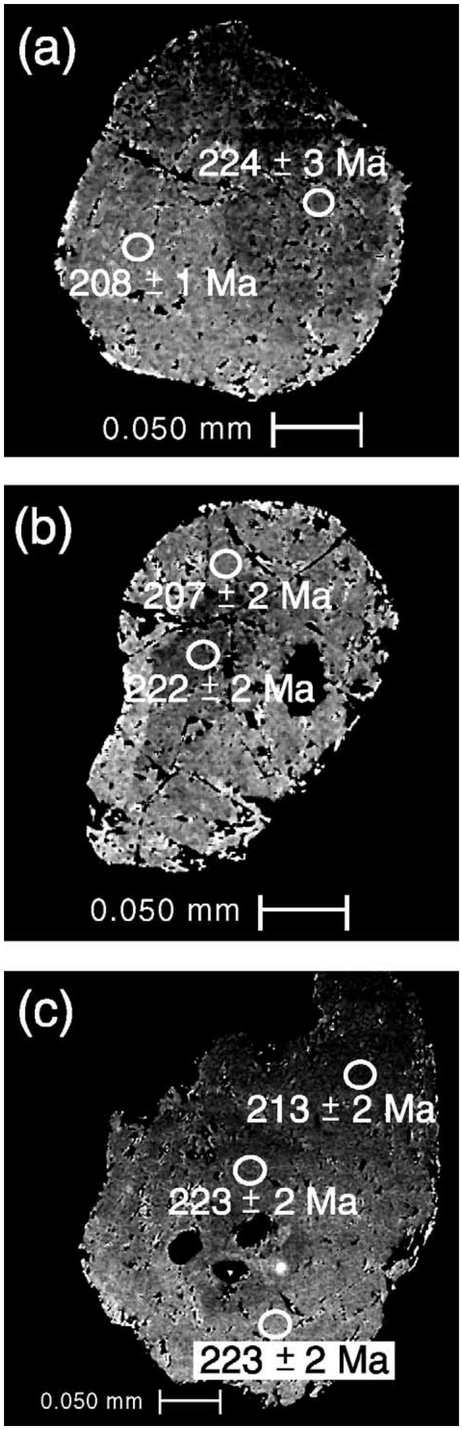

Fig. 11. BSE images of monazites from Shuanghe jadeite quartzite: (a) SH-JQ-M-32; (b) SH-JQ-M-37; and (c) SH-JQ-M-40. Ellipses mark analysis spots labeled with measured ages and 2σ errors.

4.2. Shuanghe

4.2.1. Zircons

Zircons separated from Shuanghe jadeite quartzite are generally 50–200 μm in diameter and rounded. Cathodoluminescence (Fig. 8a,c) and backscattered electron (Fig. 8b,d) images show distinct cores that occasionally display oscillatory zoning, suggestive of igneous growth, overgrown by thick homogeneous rims. Uranium concentrations in cores (median = 1500 ppm) are significantly higher than in rims (median = 340 ppm) (Table 1). The rounded shape of the grains and lack of zoning in the rims suggest that the rims are metamorphic and probably grew by coarsening (Ostwald ripening) at peak metamorphic temperature, and the thickness of the rims and relatively high U concentrations (although lower than in cores) suggest that growth may have occurred in the presence of fluid. Jadeite inclusions in the rims constrain growth to have occurred at $P > \sim 1.5$ GPa. Zircon rim analyses are all concordant and, when pooled together (Fig. 9), yield a weighted mean $^{206}Pb/^{238}U$ age of 238 ± 3 Ma ($n = 6$) with 96.7% radiogenic ^{206}Pb. Together these observations suggest that zircon growth occurred during peak UHPM at ~ 238 Ma.

Core analyses average 99.6% radiogenic ^{206}Pb and are all discordant, defining a discordia (Fig. 10) with a lower intercept age of 236 ± 32 Ma (in good agreement with pooled rim ages) and an upper intercept age of 1921 ± 23 Ma. Thus, lead loss from cores and growth of zircon rims occurred at ~ 235–240 Ma during peak UHPM conditions.

4.2.2. Monazites

Monazites separated from the Shuanghe jadeite quartzite are 50–200 μm in diameter and round or slightly elongate. Subtle core–rim zoning is apparent in backscattered electron images (Fig. 11a–c) and Ca and Th X-ray maps. Radiogenic Pb averaged 99%. Cores (223 ± 1 Ma, n= 11) are significantly older than rims, which may be composed of more than one population but, given the small number of analyses, are grouped together (209 ± 3 Ma, n = 9) with peaks in the probability plot at ~ 213 and ~ 207 Ma (Fig. 12).

5. Discussion

5.1. Growth ages or cooling ages?

The question arises as to whether measured ages correspond to cooling ages or ages of new growth and/or recrystallization? Diffusional lead loss from compositionally homogeneous grains should result in

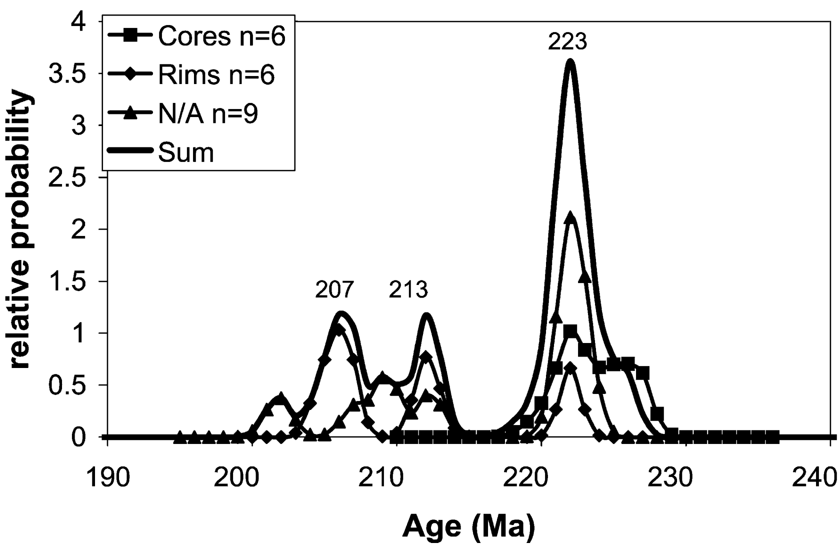

Fig. 12. Cumulative probability plot of measured $^{208}Pb/^{232}Th$ ages of Shuanghe jadeite quartzite monazites categorized as cores, rims, and uncategorized (N/A), and showing the sum of all three categories.

grains that are still compositionally homogeneous (no compositional zoning evident in backscattered electron or cathodoluminescence images) or show gradational changes in composition from core to rim, but with widely dispersed measured ages skewed to low values toward rims. These are not the characteristics observed in this study. Monazites in Shuanghe jadeite quartzite have distinct cores and rims with sharp boundaries. Distinct age differences between core (223 ± 1 Ma) and rim (209 ± 3 Ma) coupled with low variances and no significant skewness (Fig. 12) suggest that measured ages do not represent cooling ages. Recrystallization textures (patchy zoning in monazite from Maowu, Fig. 5) suggest that measured ages correspond to recrystallization-growth rather than diffusional lead loss. If rocks from Maowu and Shuanghe are from the same UHP package, and therefore experienced similar P–T–t histories, diffusional lead loss should result in similar measured age distributions. However, Shuanghe jadeite quartzite monazites record two ages, while Maowu clinopyroxenite record only one. Zircon cores in Shuanghe jadeite quartzite preserve evidence of Proterozoic crystallization, although diffusional lead loss causing discordance is evident; Maowu zircons record no ages older than ~ 235 Ma. Finally, Maowu zircons and Shuanghe jadeite quartzite zircon rims are concordant. Thus, based on textures, concordance of zircon analyses, and measured age distributions, we conclude that all measured monazite ages and concordant zircon ages represent new growth or recrystallization during Triassic subduction and exhumation. However, our conclusions remain unchanged if the ages are interpreted as cooling ages because our inferred temperatures at the time of growth, based on petrologic and petrographic observations and the interpretations of others (Table 3), are close to generally accepted estimates of closure temperatures. For example, the U/Pb closure temperature for zircon has been estimated at 750–850 °C (Heaman and Parrish, 1991) (though perfectly crystalline zircon under anhydrous conditions may have closure temperatures as high as 1000 °C for crystals of comparable size to those in this study and for reasonable cooling rates of ~ 10 °C/Ma (Cherniak and Watson, 2000)), matching the peak metamorphic temperature estimated from geothermometry for Maowu rocks (Zhang et al., 1999). This is slightly higher than our preferred estimate of 700 °C for the peak temperature for Shuanghe rocks (Liou et al., 1997), though other estimates range up to 800 ± 50 °C (Okay, 1993). Likewise, if recrystallization-growth of monazite occurred during retrograde amphibolite facies metamorphism, the corresponding temperatures of 650 °C at Maowu and 550 °C at Shuanghe (Table 4) are close to the closure temperature of ~ 670 °C for ~ 100 μm diameter grains and cooling rate of ~ 10°/Ma (Smith and Giletti, 1997).

5.2. Significance of measured ages

Another important question is whether zircon and monazite grew during peak or retrograde metamorphism? Measured ages of zircons from Maowu and Shuanghe jadeite quartzite zircon rims are in good agreement with, or slightly older than, those previously reported for Dabie Shan UHP rocks (Ratschbacher et al., 2000). Conventional TIMS U/Pb analysis of a single zircon crystal from a Shuanghe UHP metapelite yielded a concordant age of 236.4 ± 1.2 Ma (Li, 1996), in excellent agreement with our measured age of 238 ± 3 Ma for the Shuanghe jadeite quartzite. Li (1996) also measured a concordant age of 236.2 ± 2.4 Ma from a zircon from Shima (location in Fig. 1) in the southern Dabie Shan UHP zone (Wang et al., 1992). TIMS analyses of zircon from Maowu eclogite yielded a discordia with an upper intercept age of 447 + 82/ − 79 Ma and a lower intercept age of 225.5 + 3/ − 6

Table 4
P–T–t information

	Maowu	Shuanghe
Peak conditions	750 °C, 6 GPa (Zhang et al., 1999), 230 ± 4 Ma (this study)	660 °C,>2.6 GPa (Liou et al., 1997), 238 ± 3 Ma (this study)
Retrograde conditions (amphibolitization)	650 °C, 1.0–1.5 GPa (Liou and Zhang, 1998) 209 ± 2 Ma (this study)	550 °C, 1.4–1.8 GPa (Liou et al., 1997) 209 ± 3 Ma (this study)
Exhumation rate (km/Ma)	7.1–8.0	>0.94

Ma (Rowley et al., 1997). However, most of the analyses presented in Rowley et al. (1997) cluster close to concordia between 235 and 239 Ma, and $^{207}Pb/^{206}Pb$ ages cluster at 244 ± 12 Ma (2σ). Our analysis suggests that the uncertainties in the values of the upper and lower intercept ages are significantly higher than reported by Rowley et al. (1997). A Monte Carlo fit to the data using Isoplot (Ludwig, 2000) yielded a lower intercept of $224 + 34/-31$ Ma (95% C.I.), not inconsistent with our measured zircon ages of 230 ± 4 Ma for Maowu rocks and 238 ± 3 Ma for Shuanghe jadeite quartzite. Rowley et al. (1997) also dated zircons from gneisses enclosing the eclogite blocks at 218.5 ± 1.7 Ma. Hacker et al. (1998) used an ion microprobe to date zircons from host gneisses in the coesite eclogite unit and obtained a weighted mean concordia intercept age of 225 ± 4 Ma for a paragneiss and weighted mean $^{206}Pb/^{238}U$ age of 236 ± 3 Ma for an orthogneiss. Both ages are significantly older than ages measured by Rowley et al. (1997), but the age of the orthogneiss agrees well with our measured ages, while the age of the paragneiss agrees only with our measured zircon age from Maowu.

Unlike previous zircon U/Pb studies of Dabie UHP rocks (Hacker et al., 1998; Rowley et al., 1997), we found no evidence of a ~ 770-Ma component that seems to be common in gneisses of the southern Yangtze Craton and that has been interpreted as representing the timing of widespread intrusion of protolith granitoids (Rowley et al., 1997). The only pre-Triassic component observed in this study was indicated by the ~ 1.9-Ga zircon cores in the Shuanghe jadeite quartzite, and this age is consistent with a discordant age of ~ 1.9 Ga from zircon in quartzofeldspathic gneiss collected 1 m above a coesite-bearing eclogite layer from Wumiao (location in Fig. 1) in the Dabie Shan UHP zone (Marayuma et al., 1998).

Our measured zircon ages can be integrated with recent age determinations from Dabie Shan using other minerals and decay schemes. Coesite-bearing eclogite from Shuanghe yielded a garnet + omphacite + rutile Sm–Nd isochron age of 226 ± 3 Ma interpreted to represent the timing of peak metamorphism (Li et al., 2000). Gneiss from Shuanghe that hosts the eclogite blocks yielded a garnet + phengite Sm–Nd isochron age of 227 ± 3 Ma, consistent with the now widely accepted interpretation that gneisses experienced UHPM along with eclogites they host. Eclogites from Shima in the UHP zone gave a garnet + omphacite Sm–Nd isochron age of 221 ± 8 Ma (Li et al., 1993). Similarly, garnet + omphacite isochrons from eclogite and garnet peridotite from Bixiling in the Dabie Shan UHP zone (location in Fig. 1) gave Sm–Nd isochron ages of 210–218 Ma (Jahn, 1998). These ages are significantly younger than a garnet-whole rock Sm–Nd age of 246 ± 8 Ma for eclogite from the central Dabie Shan UHP zone (Okay et al., 1993). Xiao et al. (2000) interpreted coarse-grained omphacite and garnet from Bixiling to have (re)crystallized at 750–850 °C and 15–20 kbar, well below peak conditions of 1010–1090 °C and P>40 kbar estimated from K-rich omphacite inclusions in garnet, and this retrograde recrystallization may explain the younger ages reported for Bixiling by Jahn (1998). Recrystallization of garnet and omphacite in selected rocks during retrograde metamorphism may explain the wide range of Sm–Nd ages measured for Dabie Shan UHP rocks, many of which are younger than zircon ages interpreted to represent the timing of peak metamorphism. Another source of error that may lead to anomalously young garnet Sm–Nd ages is the presence of older grains of monazite included in the garnet (Koenig and Magloughlin, 2000).

Hacker et al. (1998) suggested that some zircons also recrystallize during retrograde metamorphism, with only the oldest measured ages representing the timing of peak metamorphism. Our measured zircon ages are close to the oldest ages measured by Hacker et al. (1998), so we conclude that they represent the timing of peak metamorphism at ~ 230–237 Ma. This is consistent with $^{40}Ar/^{39}Ar$ mica ages from the Hong'an region west of Dabie, which record cooling through the muscovite closure temperature between 235 and 210 Ma (Hacker et al., 2000). For the same reasons, we believe the Sm–Nd data are consistent with peak metamorphism closer to 240 than 220 Ma. Integration of $P-T-t$ estimates suggests that in some localities, such as Shuanghe and Bixiling, garnet and omphacite recrystallized during early retrograde metamorphism at ~ 220 Ma, and that evidence of peak metamorphism is preserved only in relic omphacite and coesite inclusions and in ~ 230–245 Ma zircons from this study.

Monazite seems to record multiple events during retrograde metamorphism, with Maowu mafic rocks and Shuanghe jadeite quartzite both experiencing monazite growth at ∼ 209 Ma but only the jadeite quartzite recording growth at ∼ 223 Ma. Since the pressure and temperature conditions experienced by rocks at Maowu and Shuanghe were roughly the same, only differences in composition remain to explain monazite growth in Shuanghe rocks but not Maowu rocks at ∼ 223 Ma. The ∼ 209 Ma ages may correspond to the regional amphibolite facies overprinting resulting from pervasive retrograde fluid infiltration.

According to Liou and Zhang (1998), monazite in Maowu clinopyroxenite occurs in the matrix and as inclusions in omphacite and garnet, and likely formed during metasomatic alteration at granulite facies conditions ($P = 4 \pm 2$ kbar and 730 ± 30 °C) prior to UHPM. All monazite grains in our thin sections were present on grain boundaries, and none of the monazites dated in thin section or separates record ages >225 Ma. Since recent independent estimates of the age of peak metamorphism are >225 Ma (Hacker et al., 1998), we infer that the monazites grew/recrystallized during retrograde metamorphism. Thus, monazite preserves no evidence of the early metasomatic event proposed by Liou and Zhang (1998), or of prograde or peak metamorphic conditions. Monazites included in early crystallizing phases may have preserved evidence of earlier prograde or peak metamorphic events. However, although our separates most likely contained monazites that were included in other grains, none of them yield older ages, suggesting that monazite inclusions were either occluded during retrograde metamorphism or recrystallized while occluded in another mineral.

Abundant evidence suggests that aqueous fluids retrogressed gneisses enclosing eclogite blocks at Shuanghe and Bixiling in the amphibolite facies. Oxygen isotope studies show that host gneisses and retrogressed eclogite from Bixiling have $\delta^{18}O$ 0–2.5‰, significantly lower than fresh eclogite and garnet peridotite ($\delta^{18}O$ of 3–5 ‰), suggesting that hot (meteoric?) fluids lowered $\delta^{18}O$ of host gneisses and partially retrogressed eclogite during retrograde metamorphism (Xiao et al., 2000). Fluid inclusions present in eclogite minerals suggest that fluid was present during all documented metamorphic stages, and that fluid composition evolved from Ca-rich brines during prograde metamorphism to NaCl-rich brines during peak and early retrograde metamorphism to low-salinity fluids during late retrograde metamorphism (Xiao et al., 2000). The Nd isotopic composition of garnet in granitic gneisses at Shuanghe is in equilibrium with retrogressed epidote and biotite yielding an isochron age of 213 ± 3 Ma, interpreted as the timing of fluid infiltration and amphibolitization during retrograde metamorphism (Li et al., 2000). This interpretation is consistent with peaks in our monazite age probability plots at ∼ 213 Ma for Shuanghe (Fig. 12) and ∼ 214 Ma for Maowu (Fig. 6) and our interpretation that monazite recrystallized during fluid influx. Similar ages measured for monazites from both localities (Figs. 6 and 7) suggest that this fluid infiltration event at ∼ 213 Ma was regional, and the wide spread of measured monazite ages (much greater than analytical precision, though the ages appear to represent a single population) suggests that fluid-assisted recrystallization occurred over a period of 5–10 Ma.

Our interpretation of peak UHPM at ∼ 230–237 Ma and regional retrogression at ∼ 209–213 Ma is consistent with the interpretations of Marayuma et al. (1998) based on SHRIMP analyses of zircons from a quartzofeldspathic gneiss at Wumiao in the central Dabie Shan UHP zone. In their study, homogeneous low Th/U overgrowths and whole grains yield concordant $^{206}Pb/^{238}U$ ages of 220–238 Ma, interpreted to represent growth during UHPM. Peak UHPM at ∼ 230–237 Ma coincides with the mid to late Triassic "singularity" of final coalescence of Pangea (Windley, 1995). Some zircons contain thin euhedral rims visible in CL images that yield concordant $^{206}Pb/^{238}U$ ages of 214–220 Ma, interpreted as growth or recrystallization during retrograde amphibolite facies metamorphism. A core from a concentrically zoned "dusty" zircon yielded a discordant analysis with a $^{207}Pb/^{206}Pb$ age of 1861 ± 64 Ma, similar to the upper intercept defined by discordant cores in the Shuanghe jadeite quartzite.

Conditions corresponding to peak UHPM and retrograde amphibolite facies metamorphism for Maowu and Shuanghe rocks are presented in Table 4 along with our estimates of the timing of these events. The better established pressure conditions for rocks from Maowu lead to exhumation rates of 7.1–8.0 km/Ma, and less precise estimates from Shuanghe rocks of >0.94 km/Ma, comparable to or less than modern plate velocities, which commonly reach 10 cm/year = 100 km/Ma. The exhumation rates for Maowu are consistent with >2 km/Ma estimate of Hacker et al. (2000).

Acknowledgements

Special thanks for help by Chris Coath on the UCLA ion microprobe, Alan Wiseman on the Vanderbilt SEM, and Alan Patchen on the UT Knoxville EMP. Funding was provided by NSF EAR-9873626 and a Vanderbilt University Research Council grant to Ayers:, and by the Ministry of Education of China and Chinese Ministry of Science and Technology Grant G199904320L to Gao. The University of California, Los Angeles, ion microprobe is partially subsidized by a grant from the National Science Foundation Instrumentation and Facilities Program. Thorough reviews by Brad Hacker and Simon Wilde helped to improve the manuscript. **[RR]**

References

Cherniak, D.J., Watson, E.B., 2000. Pb diffusion in zircon. Chem. Geol. 172, 5–24.

Crowley, J.L., Ghent, E.D., 1999. An electron microprobe study of the U–Th–Pb systematics of metamorphosed monazite: the role of Pb diffusion versus overgrowth and recrystallization. Chem. Geol. 157, 285–302.

Deino, A., Potts, R., 1992. Age-probability spectra for examination of single-crystal $^{40}Ar/^{39}Ar$ dating results: examples from Olorgasailie, southern Kenya rift. In: Westgate, J.A., Walter, R.C., Naeser, N. (Eds.), Tephrochronology: Stratigraphic Application of Tephra. Quaternary International Meeting, Yellowstone National Park, pp. 13–14.

Ernst, W.G., Marayuma, S., Wallis, S., 1997. Buoyancy-driven, rapid exhumation of ultrahigh-pressure metamorphosed continental crust. Proc. Natl. Acad. Sci. 94, 9532–9537.

Fitzsimmons, I.C.W., Kinny, P.D., Harley, S.L., 1997. Two stages of zircon and monazite growth in anatectic leucogneiss; SHRIMP constraints on the duration and intensity of Pan-African metamorphism in Prydz Bay, East Antarctica. Terra Nova 9, 47–51.

Hacker, B.R., Ratschbacher, L., Webb, L., Ireland, T., Walker, D., Shuwen, D., 1998. U/Pb zircon ages constrain the architecture of the ultrahigh-pressure Qinling-Dabie Orogen. China Earth Planet. Sci. Lett. 161, 215–230.

Hacker, B.R., Ratschbacher, L., Chateigner, D., 2000. Exhumation of ultrahigh-pressure continental crust in east central China: late Triassic–Early Jurassic tectonic unroofing. J. Geophys. Res. 105 (6), 13339.

Hawkins, D.P., Bowring, S.A., 1997. U–Pb systematics of monazite and xenotime: case studies from the Paleoproterozoic of the Grand Canyon, Arizona. Contrib. Mineral. Petrol. 127, 87–103.

Heaman, L., Parrish, R., 1991. U–Pb geochronology of accessory minerals. Appl. Radiogenic Isot. Syst. Probl. Geol., 59–102.

Jahn, B.-M., 1998. Geochemical and isotopic characteristics of UHP Eclogites and Ultramafic Rocks of the Dabie Orogen: implications for continental subduction and collisional tectonics. In: Hacker, B.R., Liou, J.G. (Eds.), When Continents Collide: Geodynamics and Geochemistry of Ultrahigh-Pressure Rocks. Petrology and Structural Geology. Kluwer Academic Publishing, Netherlands, pp. 203–239.

Koenig, A.E., Magloughlin, J.F., 2000. Inclusions and chemical heterogeneities in garnet: problems, pitfalls and potential for Sm–Nd geochronology. Eos Trans., Am. Geophys. Union 81 (48), F1285.

Li, S., 1996. Isotopic geochronology. In: Bolin, C. (Ed.), Ultrahigh-Pressure Metamorphic Rocks in the Dabieshan–Sulu Region of China. Petrology and Structural Geology. Kluwer Academic Publishing, Dordrecht, The Netherlands, pp. 90–105.

Li, S., Xiao, Y., Liou, D., Chen, Y., Ge, N., Zhang, Z., Sun, S.-S., Cong, B., Zhang, R., Hart, S.R., Wang, S., 1993. Collision of the North China and Yangtse Blocks and formation of coesite-bearing eclogites: timing and processes. Chem. Geol. 109, 89–111.

Li, S., Jagoutz, E., Chen, Y., Li, Q., 2000. Sm–Nd and Rb–Sr isotopic chronology and cooling history of ultrahigh pressure metamorphic rocks and their country rocks at Shuanghe in the Dabie Mountains, central China. Geochim. Cosmochim. Acta 64 (6), 1077–1093.

Liou, J.G., Zhang, R.Y., 1998. Petrogenesis of an ultrahigh-pressure garnet-bearing ultramafic body from Maowu, Dabie Mountains, east-central China. Isl. Arc 7, 115–134.

Liou, J.G., Zhang, R.Y., Wang, X., Eide, E.A., Ernst, W.G., Maruyama, S., 1996. Metamorphism and tectonics of high-pressure and ultra-high-pressure belts in the Dabie–Sulu region, China. In: Yin, A., Harrison, M. (Eds.), The Tectonic Evolution of Asia. Cambridge Univ. Press, New York, NY, pp. 300–344.

Liou, J.G., Zhang, R.Y., Jahn, B.-M., 1997. Petrology, geochemistry and isotope data on a ultrahigh-pressure jadeite quartzite from Shuanghe, Dabie Mountains, East-central China. Lithos 41, 59–78.

Liou, J.G., Zhang, R.Y., Ernst, W.G., Rumble III, D., Maruyama, S. 1998. High-pressure minerals from deeply subducted metamorphic rocks. In: Hemley, R.J. (Ed.), Ultrahigh-Pressure Mineralogy; Physics and Chemistry of the Earth's Deep Interior. Reviews in Mineralogy, pp. 33–96.

Liou, J.G., Hacker, B.R., Zhang, R.Y., 2000. Geophysics: into the Forbidden Zone. Science 287 (5456), 1215.

Ludwig, K.R., 2000. Users Manual for Isoplot/Ex: A Geochronological Toolkit for Microsoft excel Berkeley Geochronology Center Special Publication, Berkeley, CA, USA, p. 53.

Marayuma, S., Tabata, H., Nutman, A.P., Morikawa, T., Liou, J.G., 1998. SHRIMP U–Pb geochronology of ultrahigh-pressure metamorphic rocks of the Dabie Mountains, Central China. Cont. Dyn. 3 (1–2), 72–85.

Miller, C.F., Hatcher Jr., R.D., Ayers, J.C., Coath, C.D., Harrison, T.M. 2000. Age and zircon inheritance of eastern Blue Ridge plutons, southwestern North Carolina and northeastern Georgia, with implications for magma history and evolution of the Southern Appalachian Orogen. Am. J. Sci. 300 (2), 142–172.

Okay, A.I., 1993. Petrology of a diamond and coesite-bearing metamorphic terrain: Dabie Shan, China. Eur. J. Mineral. 5, 659–675.

Okay, A.I., Sengor, A.M.C., Satur, M., 1993. Tectonics of an ultrahigh-pressure metamorphic terrane: the Dabie Shan/Tongbai Shan orogen, China. Tectonics 12 (6), 1320–1334.

Poitrasson, F., Chenery, S., Bland, D.J., 1996. Contrasted monazite hydrothermal alteration mechanisms and their geochemical implications. Earth Planet. Sci. Lett. 145, 79–96.

Quidelleur, X., et al., 1997. Thermal evolution and slip history of the Renbu Zedong thrust, southeastern Tibet. J. Geophys. Res. 102, 2659–2679.

Ratschbacher, L., Hacker, B.R., Wenk, H.-R., 2000. Exhumation of the ultrahigh-pressure continental crust in east central China: cretaceous and Cenozoic unroofing and the Tan-Lu fault. J. Geophys. Res. 105 (6), 13303.

Rowley, D.B., Xue, F., Tucker, R.D., Peng, Z.X., Baker, J., Davis, A., 1997. Ages of ultrahigh pressure metamorphism and protolith orthogneisses from the eastern Dabie Shan: U/Pb zircon geochronology. Earth Planet. Sci. Lett. 151, 191–203.

Smith, H.A., Giletti, B.J., 1997. Lead diffusion in monazite. Geochim. Cosmochim. Acta 61, 1047–1055.

Stacey, J.S., Kramers, J.D., 1975. Approximation of terrestrial lead isotope evolution by a two-stage model. Earth Planet. Sci. Lett. 26, 207–221.

Tabata, H., Yamauchi, K., Marayuma, S., 1998. Tracing the extent of a UUHP metamorphic terrane: mineral-inclusion study of zircons in gneisses from the Dabie Shan. In: Hacker, B.R., Liou, J.G. (Eds.), When Continents Collide: Geodynamics and Geochemistry of Ultrahigh-Pressure Rocks. Petrol. Struct. Geol. Kluwer Academic Publishing, Dordrecht, The Netherlands, pp. 261–273.

Teufel, S., Heinrich, W., 1997. Partial resetting of the U–Pb isotope system in onazite through hydrothermal experiments; an SEM and U–Pb isotope study. Chem. Geol. 137, 273–281.

Townsend, K.J., Miller, C.F., D'Andrea, J.L., Ayers, J.C., Harrison, T.M., Coath, C.D., 2000. Low temperature replacement of monazite in the Ireteba granite, Southern Nevada: geochronological implications. Chem. Geol. 172, 95–112.

Wang, X., Liou, J.G., Marayuma, S., 1992. Coesite-bearing eclogites from the Dabie Mountains, Central China: petrogenesis, $P-T$ paths, and implications for regional tectonics. J. Geol. 100, 231–250.

Windley, B.F., 1995. The Evolving Continents Wiley, New York, NY, 526 pp.

Xiao, Y., Hoefs, J., van den Kerkhof, A.M., Fiebig, J., Zheng, Y., 2000. Fluid history of UHP metamorphism in Dabie Shan, China: a fluid inclusion and oxygen isotope study on the coesite-bearing eclogite from Bixiling. Contrib. Mineral. Petrol. 139 (1), 1–16.

Xu, S., Okay, A.I., Shouyuan, J., Sengör, A.M.C., Wen, S., Yican, L., Laili, J., 1992. Diamond from the Dabie Shan metamorphic rocks and its implication for tectonic setting. Science 256, 80–82.

Ye, K., Yao, Y., Katayama, I., Cong, B., Wang, Q., Marayuma, S., 2000. Large areal extent of ultrahigh-pressure metamorphism in the Sulu ultrahigh-pressure terrane of East China: new implications from coesite and omphacite inclusions in zircon of granitic gneiss. Lithos 52, 157–164.

Zhang, R.Y., Shu, J.F., Mao, H.K., Liou, J.G., 1999. Magnetite lamellae in olivine and clinohumite from Dabie UHP ultramafic rocks, central China. Am. Mineral. 84 (4), 564–569.